

Conf-9505122-1

SAND95-1425C

**Composition Analysis of ECR-Grown  $\text{SiO}_2$  and  $\text{SiO}_x\text{F}_y$  Films.**

**J. H. Burkhart<sup>1</sup>**

Idaho State University, Pocatello, ID 83201

**D. Denison,**

Lam Research Corporation, Fremont, CA 94538

**J. C. Barbour, and C. A. Apblett,**

Sandia National Laboratories, Albuquerque, NM 87185

Low dielectric constant insulating films, such as  $\text{SiO}_2$  and fluorine doped  $\text{SiO}_x$ , are an important class of materials in semiconductor manufacturing. Evaluation of a new process to grow low temperature  $\text{SiO}_x\text{F}_y$  films using an electron cyclotron resonance plasma (ECR) was done. Ion beam analysis techniques were used to characterize the compositions of the insulating films and correlate this with their physical and electrical properties.

Since Si, O, F, and H are of primary interest in these films three different techniques were utilized in order to get a more thorough analysis. 2.8 MeV He Rutherford Backscattering Spectrometry (RBS) revealed the Si and O content, but because of the low fluorine concentrations (2-10 at. %) RBS proved difficult for analysis of the F content. Instead, Nuclear Reaction Analysis (NRA), which used 872 keV protons in the  $^{19}\text{F}(\text{p},\alpha\gamma)^{16}\text{O}$  reaction, was employed. Finally, 30 MeV Si Elastic Recoil Detection (ERD) was used to obtain the H concentration and supplement the O analysis. The dielectric constant decreased from  $\epsilon=4$  to  $\epsilon=3.55$  as the F concentration increased from 0 to 10 %.

\* The work was partially supported by US DOE contract DE-AC04-94AL85000.

<sup>1</sup> Present address: Sandia National Laboratories, Albuquerque, NM, 87185

**DISCLAIMER**

This report was prepared as an account of work sponsored by an agency of the United States Government. Neither the United States Government nor any agency thereof, nor any of their employees, makes any warranty, express or implied, or assumes any legal liability or responsibility for the accuracy, completeness, or usefulness of any information, apparatus, product, or process disclosed, or represents that its use would not infringe privately owned rights. Reference herein to any specific commercial product, process, or service by trade name, trademark, manufacturer, or otherwise does not necessarily constitute or imply its endorsement, recommendation, or favoring by the United States Government or any agency thereof. The views and opinions of authors expressed herein do not necessarily state or reflect those of the United States Government or any agency thereof.

DISTRIBUTION OF THIS DOCUMENT IS UNLIMITED

CH

**MASTER**

## **DISCLAIMER**

**Portions of this document may be illegible  
in electronic image products. Images are  
produced from the best available original  
document.**

## 1. Introduction

Continually shrinking microelectronic device geometry has increased the need for materials with low dielectric constants that can be used as interlayer dielectrics. Low dielectric constant materials can be used to reduce the RC time constants and the overall power consumption of integrated circuits. The combination of resistance in metal interconnects and capacitance of oxide isolation layers can give sufficiently large RC time constants to limit the high-frequency response of the integrated circuit. Presently  $\text{SiO}_2$ , with a dielectric constant ( $\epsilon$ )  $\approx 4$  is the standard inter-metal dielectric, however many groups have been investigating dielectric materials with  $\epsilon \leq 3$  [1,2]. Several potential materials are being looked at including cubic boron nitride and fluorine doped  $\text{SiO}_2$ . This paper characterizes  $\text{SiO}_x\text{F}_y$  films produced by a LAM Research Corporation Electron Cyclotron Resonance (ECR) high density plasma deposition system.

Ion beam analysis techniques provide a means for quick, nondestructive composition depth profiling. The most widely available technique, Rutherford backscattering spectrometry (RBS), is useful for heavy elements on light substrates but is more difficult to use when many of the sample constituents are light elements with similar masses. One example is the analysis of F in  $\text{SiO}_2$ . For the case of F doped  $\text{SiO}_2$ , RBS can be used to ascertain the film thickness and the stoichiometry of the major constituents. However for small amounts of fluorine ( 10 atomic percent or less) nuclear reaction analysis (NRA) proves to be a more effective technique for profiling the fluorine content. NRA utilizes large, narrow reaction cross sections and a beam of varying energy to achieve good elemental sensitivity. Due to the range of incident proton energies needed to probe thick films, several resonance's often need to be accounted for in the analysis. The limit for NRA is that it is more time consuming than RBS and for the four resonance's used in this experiment it has only modest depth resolution. Finally, elastic recoil detection (ERD), will be used for the analysis of H in the F-doped samples.

## 2. Electron Cyclotron Resonance (ECR) Reactor

Figure 1 is a schematic drawing of the ECR system. The ECR consist of electromagnets which surround a plasma chamber and produce the resonance condition at 875 Gauss for 2.45 GHz microwaves. 1900 watts of 2.45 GHz microwaves where transmitted into the plasma chamber along with 112 sccm of oxygen and 120 sccm of

argon which produced the plasma. Varying combinations of  $\text{SiH}_4$  and  $\text{SiF}_4$ , with a total flow of 80 sccm, were introduced into the reaction chamber. The ratio of  $\text{SiH}_4$  to  $\text{SiF}_4$  varied from 9 to 0.1. The substrate material, in this case 8 inch Si wafers, is held in place inside of the reaction chamber by an electrostatic chuck. The substrate was held reasonably cool during deposition, around  $225^\circ \text{C}$ , using He gas as a coolant. Finally, samples had 2500 watts of RF bias placed on them. Under these conditions samples with thickness' ranging from 840 nm to 1005 nm and with fluorine content ranging from 2.4 to 10.3 atomic % were produced.

### 3. Sample Analysis

Perhaps the best known and most widely used ion beam technique is Rutherford backscattering spectrometry (RBS). This is due to the fact that RBS works well for the analysis of most elements, at least those elements that are heavier than the incident particle. Figure 2 is an example of a RBS spectra in which a 2.8 MeV He beam is scattered off of a 980 nm thick fluorine doped silicon dioxide target. The scattering angle is  $164^\circ$ , the perpendicular to the sample surface is tilted  $7^\circ$  with respect to the incident beam and the total charge collected is  $20\mu\text{C}$ . The sharp front edges of both the silicon and the oxygen signals are indicative of the excellent resolution obtainable with RBS. In general RBS provides good depth profiles, however at times a poor signal to background ratio diminishes the quality of the depth profile. Fig. 2 shows how large quantities of an element, such as oxygen in  $\text{SiO}_2(\text{F})$ , can be measured using RBS. It also illustrates how inappropriate it would be to use RBS as the sole means of analysis for this sample, since it shows no F signal and as NRA will later show this sample contains 2.4 atomic % of fluorine. Therefore, as a supplement to RBS, NRA was employed as a means to analyze the minor constituent, fluorine.

The procedure involved with NRA is rather straight forward. First one must consider which resonance to use. The  $^{19}\text{F}(\text{p},\alpha\gamma)^{16}\text{O}$  reaction has a number of resonance's to choose from [3]. All of the resonance's in the  $^{19}\text{F}(\text{p},\alpha\gamma)^{16}\text{O}$  reaction produce three gamma's which have energies of 6.13 MeV, 6.72 MeV, and 7.12 MeV. More than one of the resonance's in this reaction would have worked, but ultimately the resonance at 872 keV was chosen because it has the largest cross section, 661 mb, and yet remains reasonably narrow with a full width at half of maximum (FWHM) that is 4.5 keV. The geometry of the basic configuration is in-laid in figure 3. The

samples, which are inside of a vacuum chamber, are tilted  $15^{\circ}$  with respect to the incident beam to make the samples appear thicker and give greater depth resolution. A larger angle of tilt was avoided to prevent higher energy resonance's from dominating the analysis at the film/substrate interface. A 3 in. X 3 in. BGO detector is placed outside the chamber at an angle of approximately  $45^{\circ}$  and is approximately 5 inches from the samples. No significant attenuation of the  $\gamma$ 's is expected since these are very energetic photons that only pass through a small amount of dense material. With the accelerator off and no beam on target a spectra was taken in order to account for any background radiation. Now on the multichannle analyzer (MCA) a region of interest (ROI) was set up such that it included the gamma ray peaks, and starting at an incident proton energy well below the resonant energy, a spectra was acquired for a set amount of collected charge. The number of counts in the ROI, along with the live time was recorded. The incident proton energy was then increased by 4 or 5 keV and the process was repeated. The film thickness, which was determined earlier from RBS, was used along with the stopping power for 872 keV protons in  $\text{SiO}_2$ , which was obtained from the program TRIM [3], to determine the appropriate range over which to step the proton energies. In the energy range that was used there is a total of four resonance's that must be considered. They appear at 835 keV, 872 keV, 902 keV, and yet another at 935 keV.

Starting with a form of the Breit-Wigner [4] equation for the cross section,

$$\sigma(E) = \frac{\sigma_{res} \left( \frac{\Gamma}{2} \right)^2}{(E - E_{res})^2 + \left( \frac{\Gamma}{2} \right)^2} \quad (1)$$

where  $E_{in}$  is the incident proton energy,  $E_{res}$  is the resonant energy,  $\sigma_{res}$  is the magnitude of the cross section at  $E_{res}$ , and  $\Gamma$  is the FWHM of  $\sigma_{res}$ , an equation for the yield can be obtained. It is

$$Y = \varepsilon \Omega Q \int_{E_{in} - S_p d}^{E_{in}} \frac{c(x) \sigma(E) dE}{(Sp)} \quad (2)$$

where  $\varepsilon$  is the detector efficiency,  $\Omega$  is the solid angle subtended by the detector,  $Q$  is the number of incident protons,  $d$  is the sample thickness,  $c(x)$  is the F concentration, and  $S_p$  is the stopping power of protons in the material. The limits of the integral have been chosen such that the yield is only evaluated across the film

thickness. Assuming that the concentration and stopping power are constant and then integrating, the yield becomes

$$Y = \frac{k c \sigma_{res} \Gamma}{2 S_p} \left[ \tan^{-1} \left( \frac{2(E_{in} - E_{res})}{\Gamma} \right) - \tan^{-1} \left( \frac{2(E_{in} - E_{res} - d S_p)}{\Gamma} \right) \right] \quad (3)$$

where  $k = e\Omega Q$ . In reality the concentration may not remain constant across the sample thickness and the stopping power certainly varies some, however for the samples analyzed here the F content doesn't vary dramatically and for the energy range used and type of material being considered here, the stopping power only changes by ~5%. In the present case, where there are four resonance's involved, the yield equation becomes a sum over all four resonance's. The only adjustments that were made to the data were to subtract counts, based upon the live acquisition time, that were due to natural background radiation and that had been included in the total yield. A macro file was written using the software program Genplot [5], that would evaluate the yield equation and then plot it along with the data. Rather than calculate  $k$  it was fit using  $\text{BaF}_2$  as a calibration standard. Using a thick  $\text{BaF}_2$  sample which has a known fluorine content of 67 atomic %, and getting the stopping powers from Trim, and both  $\sigma_{res}$  and  $\Gamma$  from reference 3 or 5, the only free parameter left in the yield equation was  $k$ . This was then adjusted to find the best fit to the data. The  $\text{BaF}_2$  data and the corresponding simulated yield are shown in figure 3. Figure 4 shows the results of this analysis process as it was applied to a sample of unknown F content. This is the same  $\text{SiO}_2(\text{F})$  sample that was shown in figure 2 as an example of RBS and that showed no perceptible F content.

A third ion beam analysis technique, elastic recoil detection (ERD), is useful for light element analysis ( $1 \leq Z \leq 9$ ). The basic physical principles are similar to those of RBS, although the geometry is slightly different. In ERD the incident beam is heavier than the element to be profiled and it is incident on the target at a shallow angle. Light elements in the target will be recoiled in the forward direction, some of which will be detected. ERD also makes use of a range foil that is placed in front of the detector to filter out any of the heavier incident particles scattered toward the detector. A hydrogen profile obtained from the ERD spectra [6] of the same  $\text{SiO}_2(\text{F})$  sample shown in Fig. 2 and in Fig. 4 is shown in Fig. 5. This time a 30 MeV  $\text{Si}^{5+}$  ion beam was used to elastically recoil H atoms from the sample. The scattering angle was 30° and the beam was incident at a 15° angle to the sample surface. The resolution of the H profile is about 70 nm, and the depth of analysis was greater than the ~1050 nm

needed to profile the full  $\text{SiO}_2(\text{F})$  thickness as indicated by the ERD analysis. This compares favorably to the RBS analysis which indicated a  $\text{SiO}_2(\text{F})$  thickness of 980 nm with a resolution of 45 nm and NRA which indicated a thickness of 950 nm with a resolution of 90 nm.

#### 4. Summary

Figures 6 and 7 give an indication of how efficiently and in what manner the fluorine, which was introduced into the system in the form of  $\text{SiF}_4$ , is incorporated into the films. Figure 6 graphs  $\text{SiH}_4 / (\text{SiH}_4 + \text{SiF}_4)$  vs. % fluorine, and the results show that at least in the range studied so far, the more  $\text{SiF}_4$  introduced into the system the more F ultimately shows up in the sample. The plot inlaid in figure 7 shows the results of Fourier transform infrared (FTIR) spectroscopy on one of the films. The ratio of the peaks corresponding to the Si-O and Si-F bonds is then plotted against % fluorine, which shows that as the total amount of F in the film increases the number of Si-F bonds also increases. Finally, in figure 9, the dielectric constant of each sample is plotted against the atomic % fluorine. The data shows good agreement to a linear fit and if this relationship can be extrapolated to higher concentrations, one would expect that a dielectric constant of 3 would correspond to a fluorine content of ~24 % in this material.

Preliminary results from annealing experiments are very promising. Samples annealed in vacuum at  $450^0$  C for 3 hours show no noticeable loss of Fluorine, and a sample annealed in a nitrogen atmosphere at  $800^0$  C for 1 hour showed no degradation in electrical properties. More extensive annealing experiments are in progress and the results will be published at a later date.

[1]

[2]

[2] I. Golicheff, M. Loeuillet, and Ch. Engelmann, Journal of Radioanalytical Chemistry, 12 (1972) 233

[3] J. F. Ziegler, and J. P. Biersack, TRIM, Pergamon Press, New York (1985)

[4] J. W. Mayer, and E. Rimini, Ion Beam Handbook for Material Analysis, Academic Press, New York, (1977)

[5] Computer Graphics Services, Genplot, New York, (1989)

[6] B. L. Doyle, and D. K. Brice, NIM B35 (1988) 301

**Fig. 1.** A schematic view of the electron cyclotron resonance (ECR) system shows the basic components of the system and some of the parameters used to produce the  $\text{SiO}_x\text{F}_y$  Films studied here.

**Fig. 2.** In this example of 2.8 MeV  $\text{He}^+$  RBS a sample, which only contains a small amounts of fluorine (2.4 %), illustrates why NRA was also used, since no F signal is visible.

**Fig. 3.** The basic geometry of the NRA configuration is shown along with a plot of the data and the calculated yield curve for a bulk slab of  $\text{BaF}_2$ .

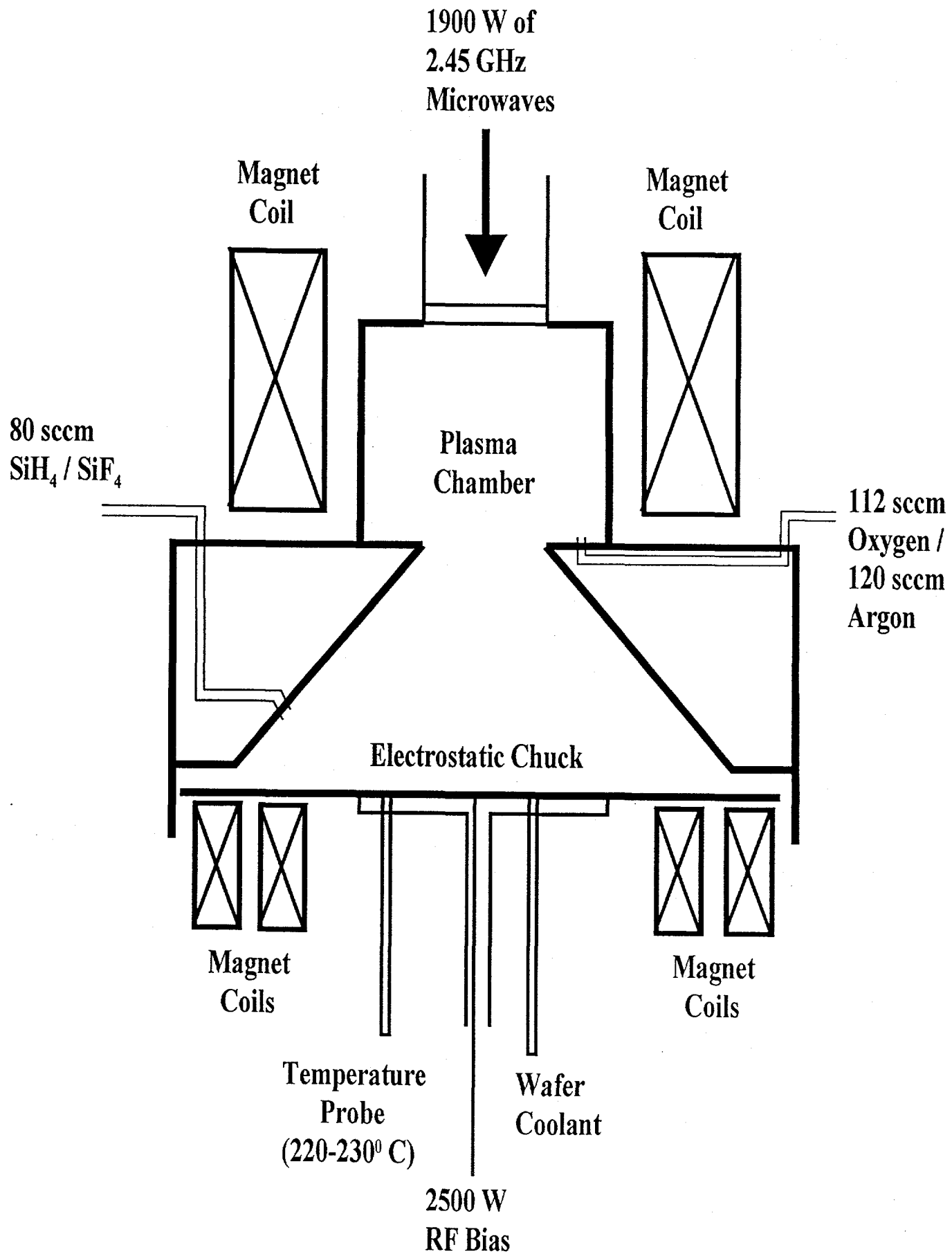
**fig. 4.** The results from NRA on a sample of unknown F content.

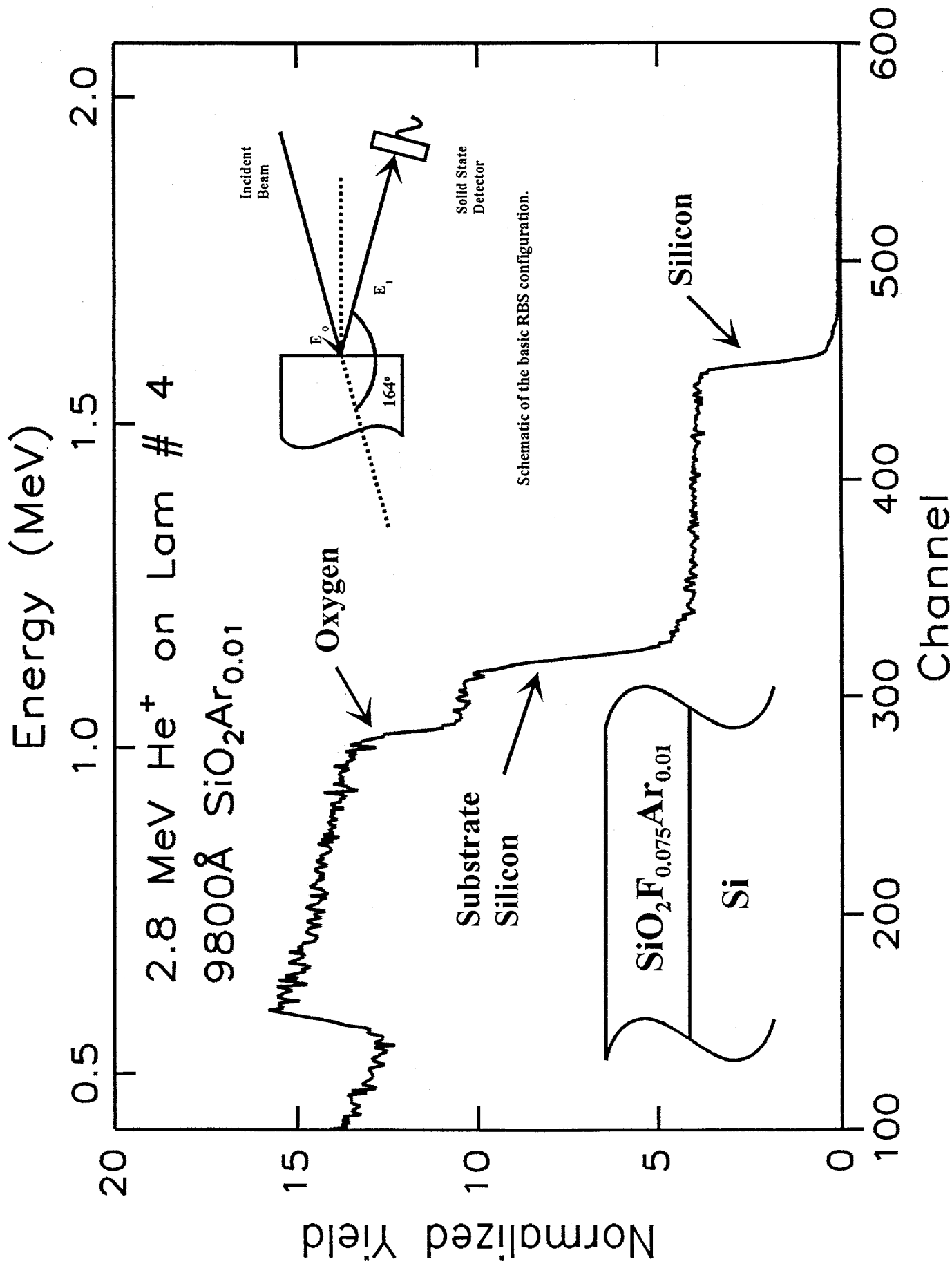
**Fig. 5.** A hydrogen profile obtained from ERD.

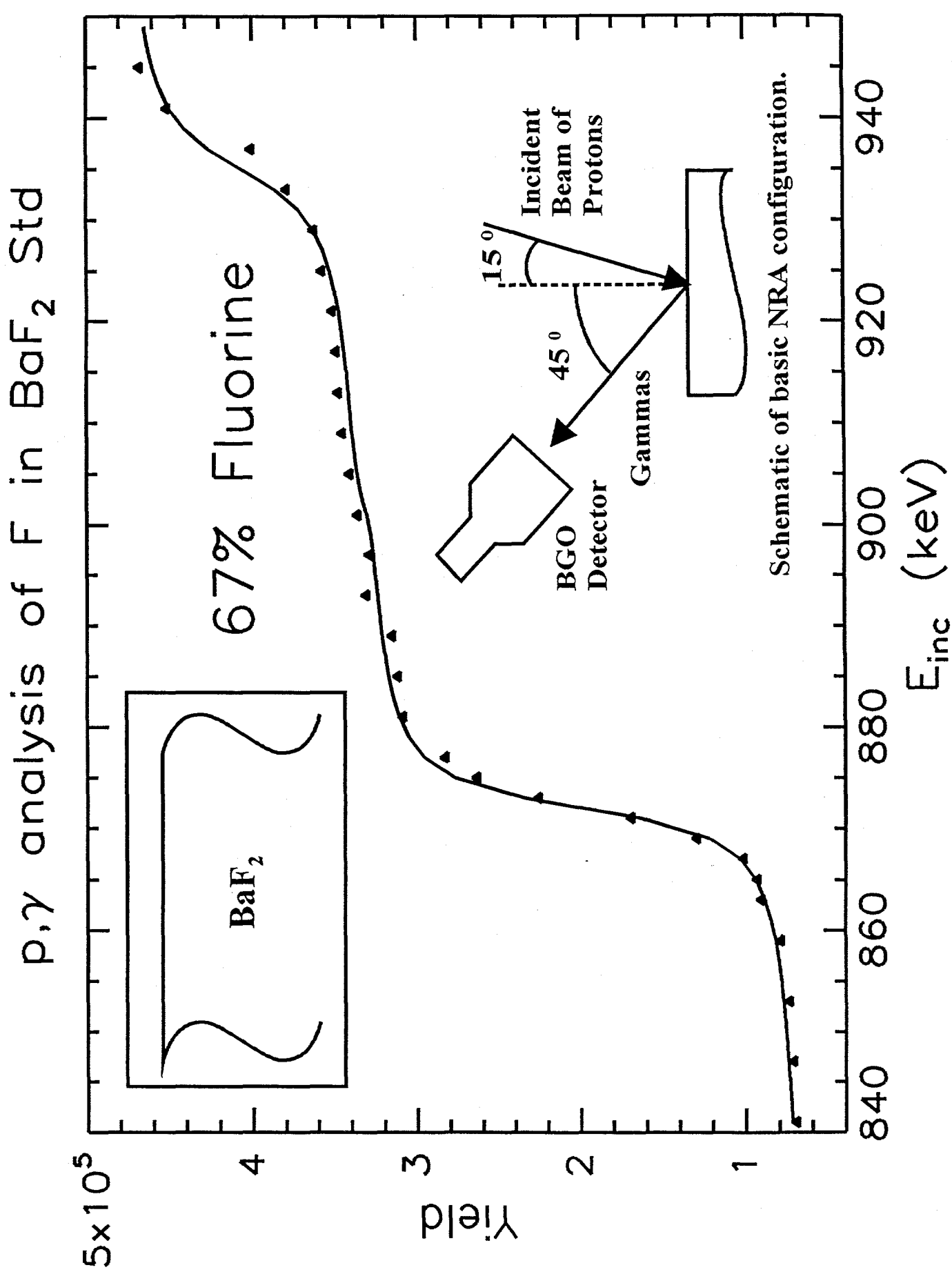
**Fig. 6.** The more  $\text{SiF}_4$  introduced into the ECR system the more F ultimately is incorporated into the Films.

**Fig. 7.** As the total amount of F in the films increases the number of Si-F bonds also increases.

**Fig. 8.** The data shows good agreement to a linear fit. Extrapolating to higher concentrations would indicate that for  $\epsilon=3$  the fluorine content would have to reach ~24 %.







p, $\gamma$  analysis of F in Lam # 4

9500Å / 2.4% Fluorine

